Multiple target tracking in seabed surveys using the GM-PHD filter

T. Fabbri*, F. Di Corato†, D. Fenucci *, D. Meucci *, A. Caiti *
*Dip. Ingegneria dell'Informazione
Università di Pisa, Pisa, Italy
Email: tommaso.fabbri@for.unipi.it
†Magneti Marelli S.p.A. - ADAS Technologies,
Venaria Reale (TO), Italy
Email: francesco.dicorato@magnetimarelli.com

***Abstract*—This paper proposes a Bayesian set-based estimator applied to the adaptive mapping of objects resting on the seabed, through the design and the implementation of a Gaussian Mixture - Probability Hypothesis Density (GM-PHD) filter. Starting from the noisy measures provided by an Autonomous Underwater Vehicle (AUV) equipped with side-scan sonar, the GM-PHD filter produces an on-line estimation of the map of the explored area. The mapping performance are demonstrated through simulations providing the effectiveness of the filter in localizing and mapping new findings and decreasing the spatial uncertainty of the position of known objects.**

Keywords—Multi-target tracking, point processes, random finite sets, intensity function, AUV, side-scan sonar.

I. Introduction

Nowadays, Autonomous Underwater Vehicles (AUVs) are able to navigate autonomously and perform a wide range of tasks. Among them, AUVs provide the capability to survey large areas of sea floor quickly while the mounted sonars produce high quality images which are able to detect most of the objects on the seabed. As matter of fact, these vehicles are used in the systematic search of objects resting on the seabed as well as during mine counter measurements[1], pipeline inspection [2] and marine archeology [3], [4]. In all these applications, there is a need to accurately determine the objects locations to build a map describing the environment. On this basis, considering the rich historical heritage of North Tyrennian Sea, starting 2011, till 2013, the Tuscany Region supported the Thesaurus Project, which long term goal was to provide marine archaeologists with technologies and methodologies for systematic search of relicts down to depths of 300m [5]. Inspired by such framework, this paper proposes a method for the adaptive mapping of a variable number of targets resting on the seabed using side-scan sonar data, through the design and the implementation of a Gaussian Mixture - Probability Hypothesis Density (GM-PHD) filter [6]. This work focuses on the feature-based approach to map, and therefore, represent in a compact and convenient way the explored environment. The estimation of the feature map thus requires the joint estimation of the number and the location of the features that have been covered by the sensor's Field of View (FOV). One of the ways to address this problem is by employing the Finite Set Statistics (FISST) [7], modeling the features state as a Random Finite Set (RFS). The recent Simultaneous Localization and Mapping (SLAM) literature [8], [9], [10], [11], shows that using the RFS theory, the mapping can be formulated as a Bayesian filtering problem where the joint posterior distribution of the feature map is propagated forward. In this paper, however, instead of propagating the full multi-target posterior density, a tractable first-order moment approximation is used, known as Probability Hypothesis Density (PHD) filter. To implement the PHD filter in an efficient and easy way, we use the Gaussian Mixture - Probability Hypothesis Density (GM-PHD) filter. As the paper will detail, the mapping algorithm is designed to account for some prior knowledge about the surveyed area. It will be shown that the algorithm is particularly robust with respect to false detections.

This paper is structured as follows. Section II describes the problem formulation and how the GM-PHD filter is casted in the working scenario. Section III outlines the implementation details, with Section IV presenting and discussing its performances. Finally, Section V summarizes the work and draws the main conclusions.

II. Problem formulation

The simulated scenario presents an Autonomous Underwater Vehicle (AUV) performing a systematic search of archaeological artifacts over a predefined Area Of Interest (AOI) using the on-board side-scan sonar. The sensor is supposed to be able to collect geo-referenced information about the visible area below the vehicle. As shown in Fig. 1, first, the data are collected and processed by a *Feature Extraction Algorithm* searching for possible features in the sonar images. Then, the *Classification Algorithm* selects object candidates among the extracted measurements. Starting from these noisy measurements an on-line estimation of the feature map of the explored area is produced. The problem of mapping the findings of archaeological interest over a predefined area can be casted as a multi-target tracking scenario where the historical artifacts are the targets and the noisy measurements provided by the classification algorithm are the inputs.

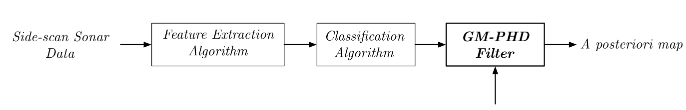

Fig. 1: Main components of the processing chain of the data collected in the simulated scenario.

978-0-933957-43-5 ©2015 MTS

In contrast to the classical multi-target tracking applications where the objective is to track a variable number of moving targets passing through the FOV of a fixed sensor, in the considered application the problem is transposed: the targets to be mapped are stationary and the sensor is moving in the AOI. Consequently, these objects can enter in or exit from the instrument FOV as the vehicle is moving.

To describe the observed pattern of points where the number of features is unknown and their identity is not important, we use a general RFS model. Following a RFS approach allows the problem of dynamically mapping multiple targets in presence of clutter and uncertainty to be cast in a Bayesian filtering problem. Let $\mathbf{X}_k$, $\mathbf{Z}_k$ be the RFSs representing the location of the known/already observed objects and the measurements received at the time k respectively, i.e.

$$\mathbf{X}_k = \{x_{k,1}, x_{k,2}, \dots x_{k,M(k)}\} \in \mathcal{F}(\mathcal{X}) \quad (1)$$
$$\mathbf{Z}_k = \{z_{k,1}, z_{k,2}, \dots z_{k,N(k)}\} \in \mathcal{F}(\mathcal{Z}) \quad (2)$$

where $\mathcal{F}(\mathcal{X})$ and $\mathcal{F}(\mathcal{Z})$ are the respective collections of all finite subsets of the target state $\mathcal{X}$ and of the measurement space $\mathcal{Z}$. Due to the limitations of the sensor involved in the considered scenario, the AUV is able to see only a sub-sector of the entire AOI. Therefore, during the exploration task the static targets will enter into and leave the FOV. To model this behavior, the RFS $\mathbf{X}_k$ can be written as:

$$\mathbf{X}_k = \mathrm{FoV}_k(\mathbf{X}_k) \cup \overline{\mathrm{FoV}}_k(\mathbf{X}_k) \quad (3)$$

where $\mathrm{FoV}_k(\mathbf{X}_k)$ and $\overline{\mathrm{FoV}}_k(\mathbf{X}_k)$ represent the tracked features inside and outside the FOV of the on-board side-scan sonar at time k respectively. We remark that the FOV depends explicitly from the time instant k as the visible area changes together with the vehicle position.
Starting from $\mathbf{X}_{k-1}$ at time $k-1$, each $x_{k-1} \in \mathrm{FoV}_k(\mathbf{X}_{k-1})$ may die or continue to exist at time k. Moreover, since the targets considered in this application are static, each $x_{k-1} \in \overline{\mathrm{FoV}}_k(\mathbf{X}_{k-1})$ continues to exist at time k. Consequently, given the multi-target state $\mathbf{X}_{k-1}$ at time $k-1$, the multi-target state $\mathbf{X}_k$ at time k is the union of the surviving targets in the FOV of the side-scan sonar $S_{k|k-1}(\mathrm{FoV}_k(\mathbf{X}_{k-1}))$, the targets outside the FOV and the spontaneous births:

$$\mathbf{X}_k = \left[\bigcup_{\zeta \in \mathrm{FoV}_k(\mathbf{X_{k-1}})} S_{k|k-1}(\zeta) \right] \cup \overline{\mathrm{FoV}}_k(\mathbf{X}_{k-1}) \cup \Gamma_k \quad (4)$$

where Γ_k is the RFS of the spontaneous births at time k used to model the new findings during the exploration. Similarly, the measurements at time k, Z_k are modeled by the RFS

$$\mathbf{Z}_k = \mathbf{K}_k \cup \left[\bigcup_{\zeta \in \mathrm{FoV}_k(\mathbf{X}_k)} \Theta(\zeta) \right] \quad (5)$$

where $\Theta(\mathrm{FoV}_k(\mathbf{X}_k))$ is the RFS of the measurements from the visible targets in $\mathbf{X}_k$, and $\mathbf{K}_k$ is a RFS used for the clutter measurements.
Let $p_k(\cdot|Z_{1:k-1})$ denote the *multi-target posterior density*, $f_{k|k-1}(\mathbf{X}_k|\mathbf{X}_{k-1})$ the *multi-target transition density* and $g_k(\mathbf{Z}_k|\mathbf{X}_k)$ the *multi-target likelihood function*, then the optimal Bayesian recursion for the multi-target model is given by [6]

$$\begin{aligned} &p_{k|k-1}(\mathbf{X}_k|\mathbf{Z}_{1:k-1}) \\ &\quad = \int f_{k|k-1}(\mathbf{X}_k|\mathbf{X}) p_{k-1}(\mathbf{X}|\mathbf{Z}_{1:k-1}) d\mathbf{X} \end{aligned} \quad (6)$$

$$p_k(\mathbf{X}_k|\mathbf{Z}_{1:k}) = \frac{g_k(\mathbf{Z}_k|\mathbf{X}_k) p_{k|k-1}(\mathbf{X}_k|\mathbf{Z}_{1:k-1})}{\int g_k(\mathbf{Z}_k|\mathbf{X}) p_{k|k-1}(\mathbf{X}_k|\mathbf{Z}_{1:k-1}) d\mathbf{X}} \quad (7)$$

The recursion Eqs. (6) and (7) involves multiple integrals making the implementation intractable for a variable number of targets. To reduce the computational complexity of propagating the multi-target posterior density, we propagate a first-order statistical moment of the posterior multi-target state through the implementation of the PHD filter [7]. For a RFS $\mathbf{X}$ on $\mathcal{X}$, the first-order statistical moment is a non-negative function $v(x)$, known as the *intensity* function [7], which integral over a region S gives the expected number of elements, $\widetilde{N}$, of the RFS $\mathbf{X}$ in the region S.

$$\widetilde{N} = \int_S v(x) dx \quad (8)$$

To realize the PHD filter the following assumptions are introduced [6]:

- Each target evolves and generates observation independently.
- Clutter is Poisson and independent of target-originated measurements.
- The predicted multi-target RFS is Poisson.

To present the PHD recursion, we introduce the followings:

$\gamma_k(\cdot)$	=	intensity of the birth Γ_k at time k.
$p_{S,k}(x_{k-1})$	=	probability that a target x_{k-1} survives at time k.
$p_{D,k}(x_{k-1})$	=	probability of detection given a state x_{k-1}.
$\kappa_k(\cdot)$	=	intensity of the clutter $\mathbf{K}_k$.

Under the assumptions introduced, the posterior intensity $v_k(x)$ can be propagated in time through the PHD recursion which can be written as

$$v_{k|k-1}(x) = \int p_{S,k}(\zeta) f_{k|k-1}(x|\zeta) v_{k-1}(\zeta) d\zeta + \gamma_k(x) \quad (9)$$

$$\begin{aligned} v_k(x) =& [1 - p_{D,k}(x)] v_{k|k-1}(x) \\ &+ \sum_{z \in \mathcal{Z}_k} \frac{p_{D,k}(x) g_k(z|x) v_{k|k-1}(x)}{\kappa_k(z) + \int p_{D,k}(\xi) g_k(z|\xi) v_{k|k-1}(\xi) d\xi} \end{aligned} \quad (10)$$

As shown in Eqs. (9) and (10), the PHD filter recursion is computationally cheaper of propagating the full posterior (Eqs. (6) and (7)). However, without further modeling assumptions the computation of the integrals do not present a closed form expression. A straightforward simplification of the foregoing recursion model is introduced by considering each individual target and the measurements as a linear Gaussian model, i.e.

$$f_{k|k-1}(x|\zeta) = \mathcal{N}(x; F_{k-1}\zeta; Q_{k-1}) \quad (11)$$
$$g_k(z|x) = \mathcal{N}(x; H_k\zeta; R_k) \quad (12)$$

where F_{k-1} is the state transition matrix, Q_{k-1} is the process noise covariance, H_k is the observation matrix and R_k is the observation noise covariance. The intensity of the birth RFS is a Gaussian mixture of the form

$$\gamma_k(x) = \sum_{i=1}^{J_{\gamma,k}} w_{\gamma,k}^{(i)} \mathcal{N}(x; m_{\gamma,k}^{(i)}; P_{\gamma,k}^{(i)}) \tag{13}$$

where $J_{\gamma,k}, m_{\gamma,k}^{(i)}, P_{\gamma,k}^{(i)}$ are model parameters. In contrast to the classical formulation [6], in this application the survival and detection probabilities are state dependent as defined in Eqs. (14) and (15).

$$p_{S,k}(x_k) = \begin{cases} p_S & \text{if the target } x_k \in \mathrm{FoV}_k(\mathbf{X}_k) \\ 1 & \text{otherwise} \end{cases} \tag{14}$$

$$p_{D,k}(x_k) = \begin{cases} p_D & \text{if the target } x_k \in \mathrm{FoV}_k(\mathbf{X}_k) \\ 0 & \text{otherwise} \end{cases} \tag{15}$$

Starting from the above assumption, the PHD propagation presents a closed form expression specified by a Gaussian mixture, known as GM-PHD. Recalling the Eq. (4), the predicted intensity and is given by

$$v_{k|k-1}(x) = v_{S,k|k-1}(x) + v_{\overline{\mathrm{FoV}}_k,k|k-1}(x) + \gamma_k(x) \tag{16}$$

where $v_{S,k|k-1}(x)$ is the intensity contribution of the surviving targets inside the FOV.

$$v_{S,k|k-1}(x) = p_{S,k} \sum_{j=1}^{J_{\mathrm{FoV}_k}} w_{k-1}^{(j)} \mathcal{N}(x; m_{S,k|k-1}^{(j)}; P_{S,k|k-1}^{(j)}) \tag{17}$$

$$m_{S,k|k-1}^{(j)} = F_{k-1} m_{k-1}^{(j)} \tag{18}$$

$$P_{S,k|k-1}^{(j)} = Q_{k-1} + F_{k-1} P_{k-1}^{(j)} F_{k-1}^T \tag{19}$$

$v_{\overline{\mathrm{FoV}}_k,k|k-1}(x)$ represents predicted mixture components of the known targets outside the FOV. In order to build an on-line map of the entire AOI during an exploration task and not losing information about the not visible features, the components $x_{k-1} \in \overline{\mathrm{FoV}}_k(\mathbf{X}_{k-1}))$ are propagated unchanged, i.e.

$$v_{\overline{\mathrm{FoV}}_k,k|k-1}(x) = \sum_{j=1}^{J_{\overline{\mathrm{FoV}}_k}} w_{k-1}^{(j)} \mathcal{N}(x; m_{k|k-1}^{(j)}; P_{k|k-1}^{(j)}) \tag{20}$$

$$m_{k|k-1}^{(j)} = m_{k-1}^{(j)} \tag{21}$$

$$P_{k|k-1}^{(j)} = P_{k-1}^{(j)} \tag{22}$$

Then, the posterior intensity at time k is also a Gaussian mixture given by

$$v_k(x) = (1 - p_{D,k}(x)) v_{k|k-1}(x) + \sum_{z \in \mathbf{Z}_k} v_{D,k}(x; z) \tag{23}$$

where the first term takes into account the miss detections of the targets in the FOV of the side-scan sonar, and the second one the contributions coming from the measurements z. For completeness the details of the update step [6] are reported below.

$$v_{D,k}(x; z) = \sum_{j=1}^{J_{k|k-1}} w_k^{(j)}(z) \mathcal{N}(x; m_{k|k}^{(j)}(z), P_{k|k}^{(j)}) \tag{24}$$

$$w_k^{(j)} = \frac{p_{D,k}(z) w_{k|k-1}^{(j)} q_k^{(j)}(z)}{\kappa_k(\zeta) + \sum_{l=1}^{J_{k|k-1}} w_{k|k-1}^{(l)} q_k^{(l)}(z)} \tag{25}$$

$$q_k^{(j)}(z) = \mathcal{N}(z; H_k m_{k|k-1}^{(j)}; R_k + H_k P_{k|k-1}^{(j)} H_k^T) \tag{26}$$

$$m_{k|k}^{(j)} = m_{k|k-1}^{(j)} + K_k^{(j)}(z - H_k m_{k|k-1}^{(j)}) \tag{27}$$

$$P_{k|k}^{(j)} = [I - K_k^{(j)} H_k] P_{k|k-1}^{(j)} \tag{28}$$

$$K_k^{(j)} = P_{k|k-1}^{(j)} H_k^T (H_k P_{k|k-1}^{(j)} H_k^T + R_k)^{-1} \tag{29}$$

In the end, to limit the number of components of the Gaussian mixture generated after each recursion, we have applied a pruning step to discard the components characterized by a weight under a predefined threshold. Then, a merging procedure based on the Mahalanobis distance [12].

III. Implementation

The GM-PHD formulation presented in Section II enables the representation of the explored AOI through a Gaussian mixture. Furthermore, the mapping algorithm is designed to account for some prior knowledge about the surveyed area. The availability of information like the expected geographical position of objects, together with qualitative information about the reliability of the indication itself and the accuracy of the referred position, let the construction of an *a priori* intensity map over the search area, which is then iteratively updated using the side-scan sonar measurements during the exploration task. In this work, we start from a historical dataset, from the archive of the National Authority describing the historical heritage of the North Tyrrhenian Sea [5]. Each entry has associated three attributes: the geographical position x_i of the entry representing the specific position on the map where the finding was discovered; the reliability $w_0^{(i)}$ of the indication and the uncertainty $\sigma_0^{2,(i)}$. The dataset $\mathbb{X} = \{X_i\}$ of N_0 points where each entry is a triple of attributes encoding the spatial and qualitative information.

$$X_i(x_i; w_0^{(i)}; \sigma_0^{2,(i)}) \qquad i = 1, \ldots, N_0 \tag{30}$$

In this application, the dataset $\mathbb{X}$ is recast to fit the Gaussian mixture to obtain an a priori description of the environment. The reliability is recast into the weight of the mixture components. The value of this attribute was rescaled into the range $[0, 1]$ to represent the peak of the Gaussian. The remaining parameters x_i and $\sigma_0^{2,(i)}$ naturally adapt to the mean and variance of each component. Fig. 2 shows the locations x_i of the findings on a map of the North Tyrrhenian Sea. Fig. 3 illustrates the intensity map computed as a Gaussian mixture from the dataset $\mathbb{X}$. The hot colors indicate high concentration of findings on the seabed while cold colors indicate low concentration. In the simulated scenario, an AUV explores the AOI following a lawnmower trajectory to produce an intensity map of the area explored. The AUV is modeled as a kinematic point, able to perfectly follow the planned trajectory at a fixed speed of 2 m/s and with a fixed distance from the sea-bottom

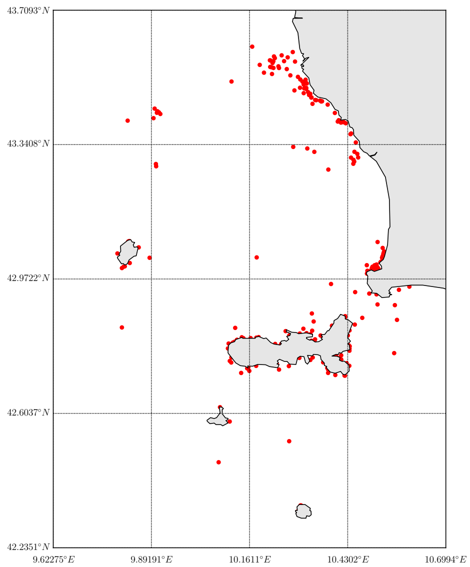

Fig. 2: Plot of the historical dataset from the National Authority of the North Tyrrhenian Sea.

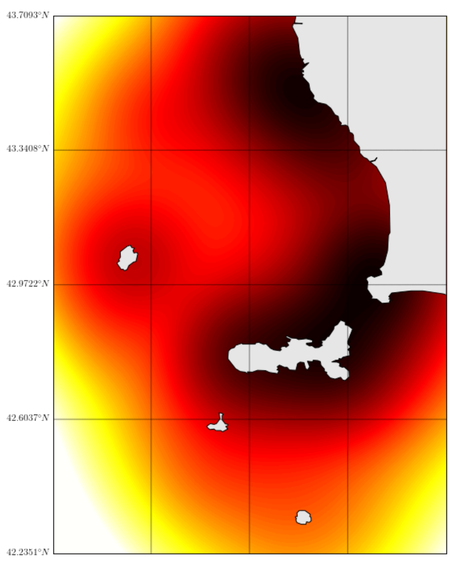

Fig. 3: Intensity map of the North Tyrrhenian Sea. Hot colors indicate regions characterized by high density of objects on the seabed, while cold colors represent low density.

of 100 m. The side-scan sonar considered in the simulations is modeled on the basis of the Tritech® SeaKing characteristics [13], which is able to scan an area of $\approx 600\,\mathrm{m}^2$ at each time step. The blind zone on the nadir caused by the geometry of the emitted beams develops below the vehicle and it extends for 114 m, as shown in Fig. 4. Each time the AUV passes over in the object on the seabed, and the object enters in the FOV, the simulated system may generate a *feature report* and then a *classification report*, containing the measured location of the feature. The likelihood of a feature report and the likelihood of a correct classification are dependent on various parameters (e.g. sensor settings, relative angle, properties of the object).

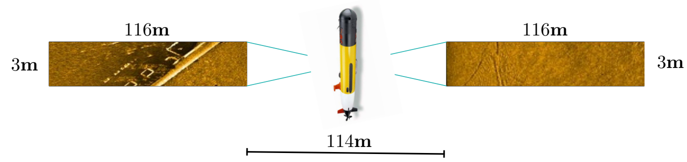

Fig. 4: Area covered by the Tritech® SeaKing side-scan sonar at each time step (image not in scale for reading purpose).

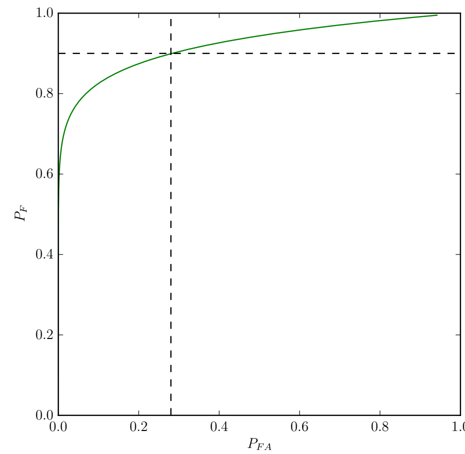

Fig. 5: Simulated Feature Extraction Algorithm Receiver Operating Characteristic

Each time an object enters into the FOV, the system makes a feature determination based on:

- If the object is a real target (relict) the Feature Extraction Algorithm will report a detection with probability P_F.
- If the object is a false alarm the Feature Extraction Algorithm will report a false detection with probability P_{FA}

Fig. 5 shows the Receiver Operating Characteristic (ROC) of the simulated Feature Extraction Algorithm and an example of the selected thresholds ($P_F = 0.9$ and $P_{FA} = 0.28$). Once a detection has been made for an object, the object is processed by the simulated Classification Algorithm. The simulator makes a classification determination based on the value of P_C.

- If the object is a relict, the Classification Algorithm will report it as relict with probability P_C.
- If the object is a false alarm, the Classification Algorithm will discard the extracted feature with probability P_C.

IV. Simulation Results

The simulation scenario is represented by a region of $80\,\mathrm{km} \times 160\,\mathrm{km}$ width where the targets from the dataset $\mathbb{X}$ are located. Despite the practical issues that a survey in such a wide area would imply (e.g. mission duration, power consumption), the simulations were performed considering the whole area in order to exploit the full historical dataset. Each target follows the linear Gaussian dynamics, Eq. (11), with

$$F_k = I_2 \qquad\qquad Q_k = \sigma_p^2 I_2 \tag{31}$$

where I_2 denotes a 2×2 identity matrix, with $\sigma_p = 0.001$ the standard deviation of the process noise. The σ_p is characterized by a low value because of the static nature of the targets involved in the simulated scenario. The measurement follows the observation model Eq. (12), with

$$H_k = I_2 \qquad\qquad R_k = \sigma_\epsilon^2 I_2 \tag{32}$$

where $\sigma_\epsilon = 1.5$ is the standard deviation of the measurement noise. At every simulation run, a partial knowledge of the AOI is provided as a random subset of 20 entries of $\mathbb{X}$ to build the *a priori* intensity map. Fig. 7a shows an example of the *a priori* intensity map. The *a priori* map is characterized by high spatial uncertainty making the map unusable in practical searching applications. As matter of fact, the uncertainty ranges between 5 km to 10 km. The real targets are immersed in a set of false alarms equally distributed along the AOI. Fig. 6 shows positions of the real targets, from the historical database, and the set of 250 false alarms randomly generated.

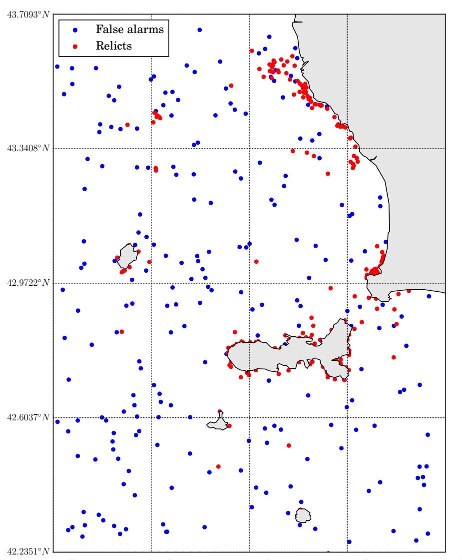

Fig. 6: Plot of the targets to be tracked (red circles) from the dataset $\mathbb{X}$ and the set of false alarms (blue circle) randomly generated.

During the exploration task, the AUV follows a lawnmower trajectory to scan the entire AOI; at each scan, the GM-PHD filter uses the field measurements to update the state of known targets or to track new discovered ones. Figs. 7b and 7c present the resulting *posterior* intensity map and the extracted target positions, respectively. Comparing Figs. 7a and 7b, the filter is able to localize and map new findings and decrease the spatial uncertainty of known targets. Furthermore, comparing Fig. 3 representing the *a priori* full knowledge of the entire AOI with Fig. 7b we can notice that through the use of the GM-PHD during an exploration task, the spatial uncertainty can be radically reduced. Fig. 7c shows that the proposed approach is able not only to detect and track the new discovered relicts, but also to filter the false alarms.

V. Conclusions and Future Work

This work presented a Bayesian set-based estimator applied to the adaptive mapping of objects resting on the seabed though the use of field measures from a side-scan sonar during an exploration task. Simulations demonstrated the GM-PHD filter is able to localize and track new findings and consequently generate on-line map update. Furthermore, the filter is designed to account for some prior knowledge about the surveyed area. Future works will be focused on the application of the proposed approach to cooperative exploration algorithms of team of AUVs, in order to adapt the cooperative mission based on new findings.

References

[1] R. Stokey, T. Austin, B. Allen, N. Forrester, E. Gifford, R. Goldsborough, G. Packard, M. Purcell, and C. von Alt, "Very shallow water mine countermeasures using the remus auv: a practical approach yielding accurate results," in *OCEANS, 2001. MTS/IEEE Conference and Exhibition*, vol. 1, 2001, pp. 149–156 vol.1.

[2] Y. Petillot, S. Reed, and J. Bell, "Real time auv pipeline detection and tracking using side scan sonar and multi-beam echo-sounder," in *OCEANS '02 MTS/IEEE*, vol. 1, Oct 2002, pp. 217–222 vol.1.

[3] F. Di Corato, D. Meucci, and A. Caiti, "Information-driven cooperative distributed motion planning for long range search over marine areas," in *Proceedings of 3rd IFAC Workshop on Multivehicle Systems MVS 2015*, Genova, Italy, 2015.

[4] A. Caiti, V. Calabro, F. Di Corato, T. Fabbri, D. Fenucci, A. Munafo, B. Allotta, F. Bartolini, R. Costanzi, J. Gelli, N. Monni, M. Natalini, L. Pugi, and A. Ridolfi, "Thesaurus: Auv teams for archaeological search. field results on acoustic communication and localization with the typhoon," in *Control and Automation (MED), 2014 22nd Mediterranean Conference of*, June 2014, pp. 857–863.

[5] B. Allotta, S. Bargagliotti, L. Botarelli, A. Caiti *et al.*, "Thesaurus project: Design of new autonomous underwater vehicles for documentation and protection of underwater archaeological sites," in *Progress in Cultural Heritage Preservation*, ser. Lecture Notes in Computer Science, M. Ioannides, D. Fritsch, J. Leissner, R. Davies, F. Remondino, and R. Caffo, Eds. Springer Berlin Heidelberg, 2012, vol. 7616, pp. 486–493. [Online]. Available: http://dx.doi.org/10.1007/978-3-642-34234-9_50

[6] B.-N. Vo and W.-K. Ma, "The gaussian mixture probability hypothesis density filter," *Signal Processing, IEEE Transactions on*, vol. 54, no. 11, pp. 4091–4104, Nov 2006.

[7] R. Mahler, "Multitarget bayes filtering via first-order multitarget moments," *Aerospace and Electronic Systems, IEEE Transactions on*, vol. 39, no. 4, pp. 1152–1178, Oct 2003.

[8] D. Moratuwage, D. Wang, A. Rao, N. Senarathne, and H. Wang, "Rfs collaborative multivehicle slam: Slam in dynamic high-clutter environments," *Robotics Automation Magazine, IEEE*, vol. 21, no. 2, pp. 53–59, June 2014.

[9] J. Mullane, B.-N. Vo, M. Adams, and B.-T. Vo, "A random-finite-set approach to bayesian slam," *Robotics, IEEE Transactions on*, vol. 27, no. 2, pp. 268–282, April 2011.

[10] J. Mullane, B.-N. Vo, and M. Adams, "Rao-blackwellised phd slam," in *Robotics and Automation (ICRA), 2010 IEEE International Conference on*, May 2010, pp. 5410–5416.

[11] C. S. Lee, D. Clark, and J. Salvi, "Slam with single cluster phd filters," in *Robotics and Automation (ICRA), 2012 IEEE International Conference on*, May 2012, pp. 2096–2101.

[12] P. C. Mahalanobis, "On the generalised distance in statistics," in *Proceedings National Institute of Science, India*, vol. 2, no. 1, Apr. 1936, pp. 49–55. [Online]. Available: http://ir.isical.ac.in/dspace/handle/1/1268

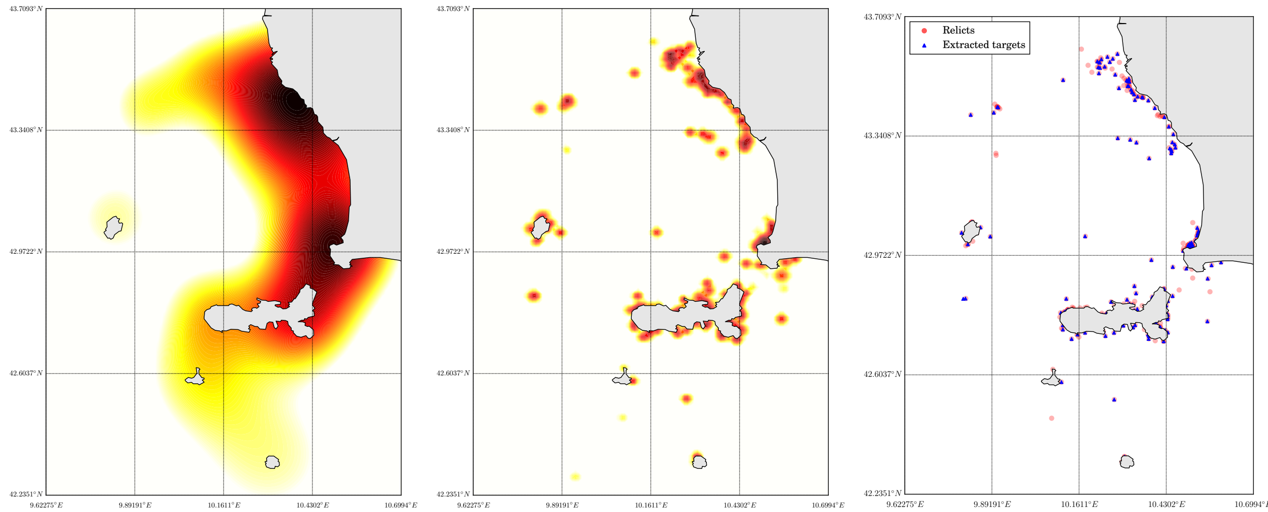

(a) *A priori* intensity map. (b) *Posterior* intensity map. (c) Extracted targets.

Fig. 7: Results of the exploration task: Fig. 7a represents the *a priori* intensity map generated from 20 entries of the dataset $\mathbb{X}$; the map is characterized by high spatial uncertainty. Fig. 7b shows the *posterior* intensity map generated at end of the exploration task; the spatial uncertainty is radically reduced and new targets are detected and tracked. Fig. 7c represents the positions of the real targets and the extracted ones; the filter is able to detect and track new targets and discard correctly the false alarms.

[13] "Tritech SeaKing side-scan sonar," http://www.tritech.co.uk/product/side-scan-sonar-seaking-auv-rov.